 doi:10.20944/preprints202011.0408.v1

Article

Inhibition of Pneumolysin Cytotoxicity by Hydrolyzable Tannins

Santeri Maatsola [1], Sami Kurkinen [2], Marica T. Engström [3], Thomas K.M. Nyholm [4], Olli Pentikäinen [5], Juha-Pekka Salminen [6] and Sauli Haataja[7]*

1 Institute of Biomedicine, Research Center for Cancer, Infections and Immunity, University of Turku, Finland;sjjmaa@utu.fi
2 Institute of Biomedicine, Integrative Physiology and Pharmacology, University of Turku, Finland; sami.t.kurkinen@utu.fi
3 Natural Chemistry Research Group, Department of Chemistry, University of Turku; Institute of Biomedicine, Bioanalytical Laboratory, University of Turku, Finland mtengs@utu.fi
4 Biochemistry Faculty of Science and Engineering, Abo Akademi University, Turku, Finland; Thomas.Nyholm@abo.fi
5 Institute of Biomedicine, Integrative Physiology and Pharmacology, University of Turku, Finland; olli.pentikainen@utu.fi
6 Natural Chemistry Research Group, Department of Chemistry, University of Turku; j-p.salminen@utu.fi
7 Institute of Biomedicine, Research Center for Cancer, Infections and Immunity, University of Turku, Finland; sauli.haataja@utu.fi
* Correspondence: sauli.haataja@utu.fi

Abstract: *Streptococcus pneumoniae* causes invasive infections such as otitis media, pneumonia and meningitis. It produces pneumolysin (Ply) toxin, which forms a pore to host cell membrane and has multiple functions in *S. pneumoniae* pathogenesis. The Ply C-terminal domain 4 mediates binding to membrane cholesterol and induces the formation of pores composed of up to 40 Ply monomers. Ply has a key role in the establishment of nasal colonization, pneumococcal transmission from host to host and pathogenicity. Altogether, 27 hydrolyzable tannins were tested for Ply inhibition in hemolysis assay and tannin-protein precipitation assay. Pentagalloylglucose (PGG) and gemin A showed nanomolar inhibitory activity. Ply oligomerization on the erythrocyte surface was inhibited with PGG. PGG also inhibited Ply cytotoxicity to A549 human lung epithelial cells. Molecular modelling of Ply interaction with PGG suggested that it binds to the pocket formed by domains 2, 3 and 4. In this study, we reveal the structural features of hydrolyzable tannins that are required for interaction with Ply. Monomeric hydrolysable tannins containing a sufficient number of polyvalent and flexible galloyl groups have highest inhibitory power to Ply cytotoxicity, and are followed by oligomers. Of the oligomers, macrocyclic and C-glycosidic structures were weaker in their inhibition than the glucopyranose-based oligomers. Accordingly, PGG-type monomers and certain oligomers might have therapeutic value in the targeting of *S. pneumoniae* infections.

Keywords: *Streptococcus pneumoniae*; pneumolysin; tannins; pentagalloylglucose; gemin A

1. Introduction

Streptococcus pneumoniae is a major cause of human pneumonia, otitis media and meningitis. It is estimated that it causes globally over 500,000 deaths every year. *S. pneumoniae* has multiple virulence factors which contribute to its adhesion to the host nasopharyngeal mucosal surfaces, escape from immune defence mechanisms and invasion to host tissues [1]. Due to the emergence of antibiotic resistance and replacement of serotypes included in the current vaccines with non-vaccine serotypes, the global burden of *S. pneumoniae* infection remains a serious problem [2,3]. Development of alternative non-bacteriosidic compounds, which would prevent infections, are needed.

Preprints (www.preprints.org) | NOT PEER-REVIEWED | Posted: 16 November 2020 doi:10.20944/preprints202011.0408.v1

Compounds that will target bacterial *in vivo* virulence factors essential for survival in the host, such as pneumolysin (Ply), are candidates that could be used in the prevention of infections.

Pneumolysin is a 53 kDa protein of *S. pneumoniae,* belonging to the family of cholesterol-dependent cytolysins (CDC) [4]. Upon interaction with eukaryote membrane cholesterol, pneumolysin is oligomerized, and it creates a pore into the membrane and kills the target cell. It is composed of 4 distinct domains. Domains 1, 2, and 3 are required for oligomerization and domain 4 is responsible for host cell recognition and cholesterol binding [5]. Unlike the other members of the CDC toxin family, Ply has no signal peptide for secretion and is released from the bacterial cytoplasm by autolysis and allolysis during the natural competence for DNA transformation [6]. Ply has also been shown to be secreted by accessory SecY2A2 Sec system and is found in the active form attached to the pneumococcal cell wall [7,8]. Ply is a highly multifunctional toxin, which in addition to its hemolytic and cytolytic activity can cause pyroptosis, apoptosis, regulate complement activity, induce a number of signalling effects and also play a role in *S. pneumoniae* transmission from host to host [9–11]. Since Ply contributes to *S. pneumoniae* survival throughout its presence in the host (i.e. colonization, infection and transmission), it is an important target for the prevention of pneumococcal infections.

Tannins can be classified to condensed tannins (syn. proanthocyanidins), hydrolysable tannins and phlorotannins as reviewed by Quideau et al. [12]. They are highly versatile plant polyphenols important to host defence mechanisms against pathogens, and as scavengers of UV-B light and highly reactive oxidative radicals [12]. Functionally tannins can react with proteins by binding with them as multidentate ligands, ultimately leading to the precipitation of tannin-protein complexes, thereby reducing the nutritional value of plants to pathogens. The phenolic rings can interact with proteins by forming hydrophobic interactions by π-stacking with aromatic side-chains of protein and via van der Waals interactions. The phenolic hydroxy-groups can interact by forming hydrogen bonds and dipole-dipole interactions.

Recently, epigallogatechin gallate (EGCG) was shown to inhibit pneumolysin hemolysis and cytotoxicity [13]. This compound is a gallic acid ester of a flavan-3-ol monomer. Interestingly, all hydrolysable tannins consist of this same gallic acid moiety esterified typically to a sugar-type polyol and are modified further e.g. by oxidative reactions to yield almost 1000 monomeric and oligomeric structures. All these can be purified and studied as individual compounds, unlike proanthocyanidins and phlorotannins that typically are complex mixtures of their polymeric forms [14–16]. Here, we purified 27 hydrolyzable tannins and studied how they could inhibit Ply cytotoxicity. We show that the hemolysis, Ply oligomerization and cytotoxicity of Ply is inhibited with hydrolyzable tannins. The structure-activity relationship suggests that the polyvalency and flexibility of the galloyl groups and the formation of flexible oligomers increase the inhibitory power of these tannins.

2. Results and discussion

2.1. Inhibition of hemolysis by hydrolyzable tannins

27 hydrolyzable tannins (Figure 1 and 2, Table A1) were tested for their inhibitory activity against pneumolysin hemolytic activity. Inhibition assay performed with the two-fold dilutions of tannins classified the compounds to three groups; negative or weak inhibitors (IC_{50} ≥ 100 nM), moderate inhibitors (IC_{50} 40 - 90 nM) and potent inhibitors (IC_{50} 10 - 30 nM). These results alone suggested that the inhibitory activity of hydrolysable tannins could be linked to their capacity to bind with Ply; the inhibitory activities quite closely followed the protein precipitation capacity patterns earlier detected for these tannins [15]. For the monomers, a good number of flexible galloyl groups was critical to the activity, while for oligomers both flexibility and glucopyranose-based cores structure was important. The non-flexible macrocyclic oenothein B and the C-glycosidic oligomers salicarinins A, B and C were the weakest of the oligomers. Pentagalloylglucose (PGG), the most active monomer, and gemin A, the most active oligomer, were chosen for more extensive characterization

Preprints (www.preprints.org) | NOT PEER-REVIEWED | Posted: 16 November 2020 doi:10.20944/preprints202011.0408.v1

of the inhibitory properties of these compounds. Moderate and weak inhibitors oenothein B (oligomer) and vescalagin (monomer) were chosen as control compounds.

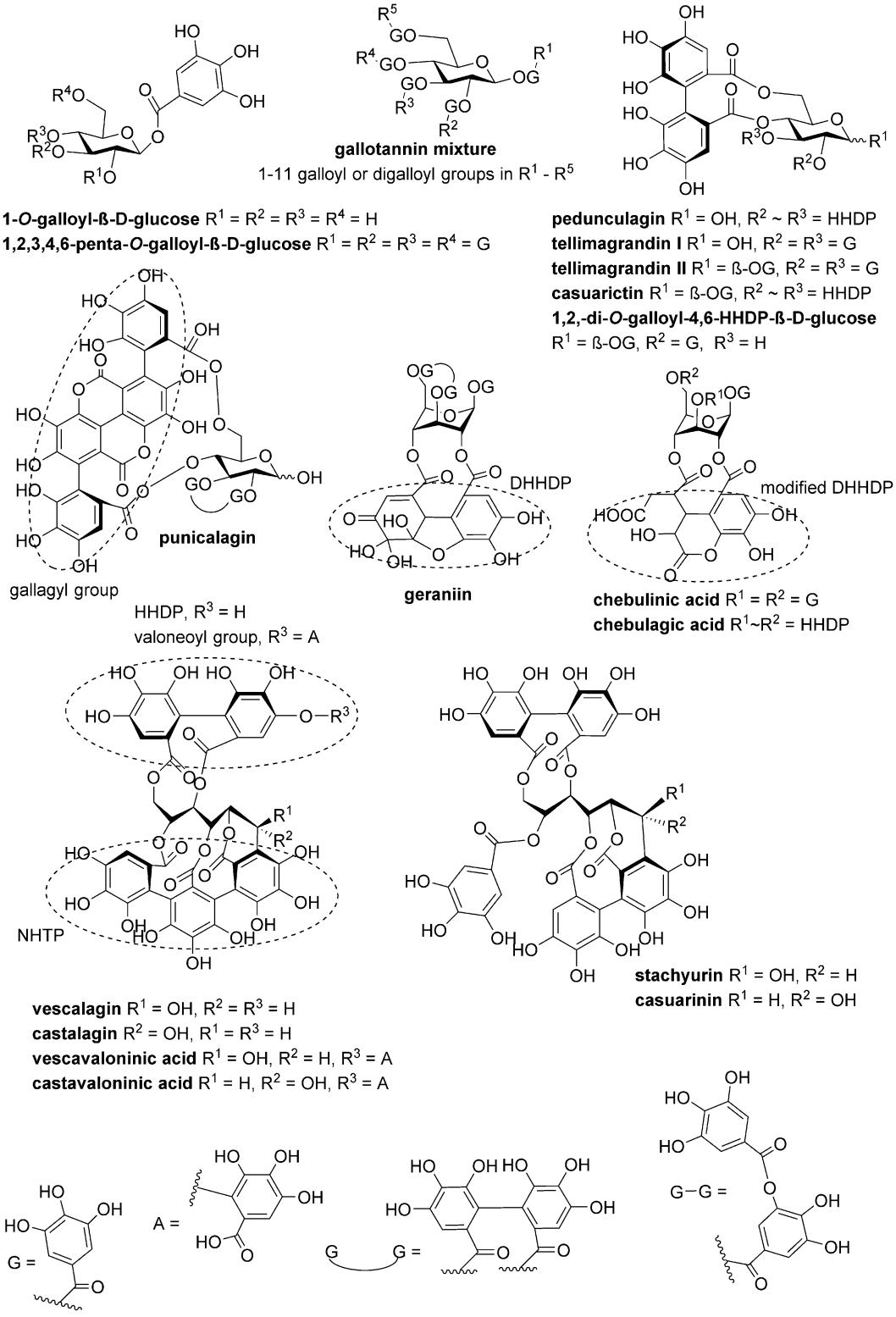

Figure 1. The structures of the monomeric tannins used in this study.

Preprints (www.preprints.org) | NOT PEER-REVIEWED | Posted: 16 November 2020 doi:10.20944/preprints202011.0408.v1

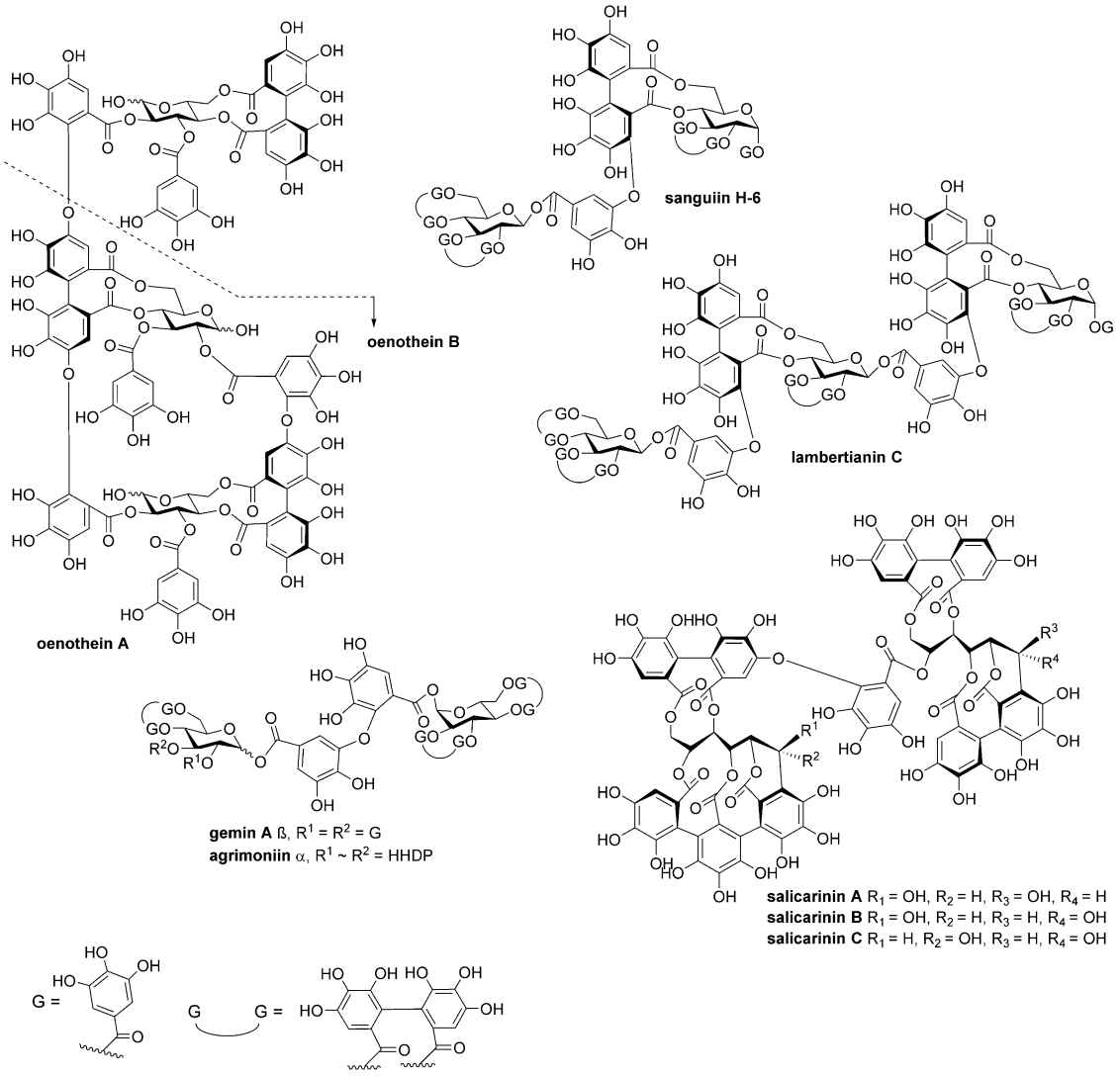

Figure 2. The structures of the oligomeric tannins used in this study.

2.2. Inhibitory power of PGG and Gemin A

The tannin concentrations giving 50 % inhibition (IC_{50}) of hemolysis were determined (Figure 3). PGG had an IC_{50} of 18±0.7 nM and inhibitory power of 13 compared to vescalagin (IC_{50} of 240±5.3 nM and inhibitory power 1). The inhibitory power of gemin A was 5.9, and oenothein B was 4.4 (IC_{50} 41±1 nM and 55±2.1 nM, respectively). The most potent compound causing precipitation was gemin A. Its potency to cause precipitation was 130-fold compared to vescalagin. In contrast, PGG was two-fold weaker compared to gemin A but was still 58-fold stronger compared to vescalagin (Figure 4). These results followed quite accurately the precipitation results obtained with BSA protein [15] , suggesting that the structure-activity patterns found in that study for 32 purified hydrolysable tannins could be valid against Ply as well as BSA.

Preprints (www.preprints.org) | NOT PEER-REVIEWED | Posted: 16 November 2020 doi:10.20944/preprints202011.0408.v1

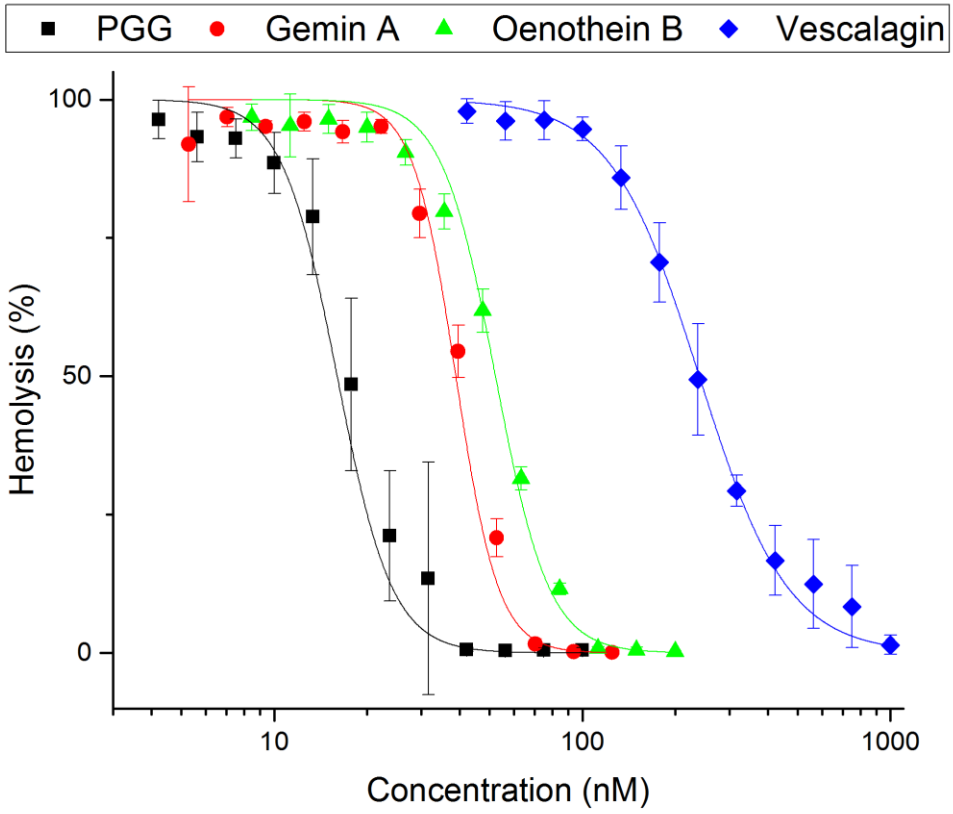

Figure 3. The inhibition of pneumolysin activity by tannins. The hemolysis caused by Ply was analyzed based on the release of hemoglobin from the lysed erythrocytes. The haemoglobin was quantitated based on its absorbance at 570 nm (triplicate measurements). The %-hemolysis values are shown in the y-axis as a function of inhibitor concentration (x-axis). IC_{50} values for representative polyphenols were calculated with Origin.

Preprints (www.preprints.org) | NOT PEER-REVIEWED | Posted: 16 November 2020 doi:10.20944/preprints202011.0408.v1

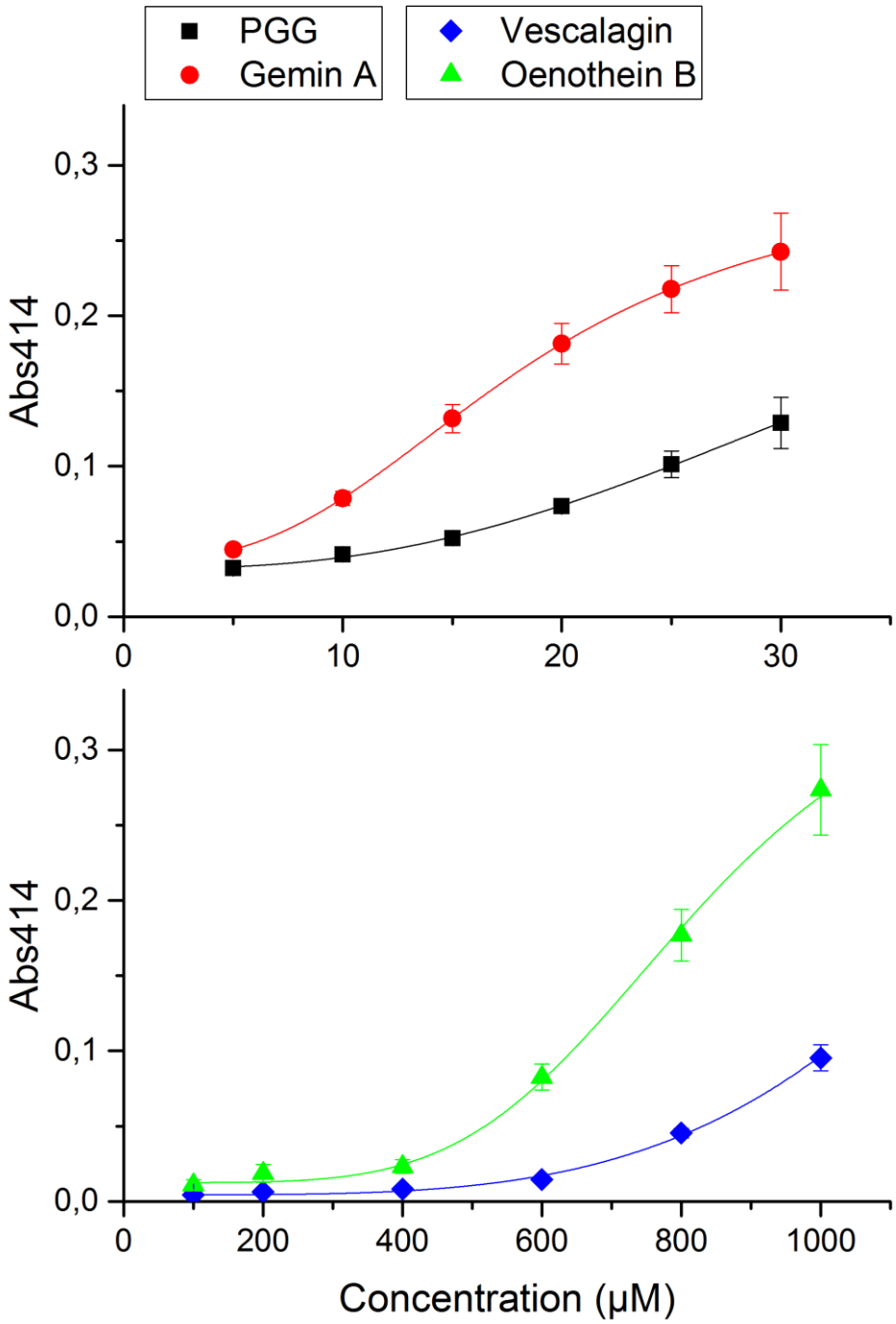

Figure 4. Precipitation assay of pneumolysin – tannin interaction. The precipitation caused by tannins were analyzed by measurement of the absorbance at 414 nm. The minimum concentration still precipitating Ply was calculated.

The hemolysis inhibition and the precipitation assay results were compared (Table 1). The results show that both of these assays correlate to each other, however, the precipitation required 1000-fold higher concentrations (µM vs nM) to cause the effect. This was expected, since the precipitation assay measures the insoluble complex formed at high tannin to protein ratio. Below these concentrations tannins are known to first form soluble complexes with proteins. This presumably took place in the hemolysis inhibition assay. The inhibition of hemolysis by tannins could

Preprints (www.preprints.org) | NOT PEER-REVIEWED | Posted: 16 November 2020 doi:10.20944/preprints202011.0408.v1

be based on the blocking of Ply binding to erythrocytes and by direct binding to the Ply domains contributing to the oligomerization of Ply. Interestingly, also the potency of oenothein B and vescalagin to cause pneumolysin precipitation correlated to the inhibitory power in hemolysis inhibition assay. Since the essential property of pneumolysin is to oligomerize, therefore the inhibitory mechanism of tannins could be based on targeting the domains that are required for the oligomerization.

Table 1. Comparison of the hemolysis inhibition and tannin precipitation powers of selected hydrolysable tannins.

Compound	Hemolysis inhibition		Minimum precipitating concentration	
	IC_{50} [nM]	Inhibitory power	[μM]	Relative power
PGG	18 ± 0,7	13	14	58
Gemin A	41 ± 1,0	5,9	6,2	130
Oenothein B	55 ± 2,1	4,4	510	1,6
Vescalagin	240 ± 5,3	1	820	1

2.3. PGG abolishes oligomerization of pneumolysin

Ply oligomerization assay was developed using erythrocytes as target cells. Ply recognizes cholesterol on the erythrocyte cell surface, which initiates a cascade of events that results in the membrane pore formation and subsequent cell lysis. The large 2500 kDa Ply complex can be recognized when the isolated membranes are dissolved into SDS-PAGE sample buffer (Figure 5AB) and the membrane-bound proteins are separated on the SDS-PAGE gel. PGG was tested for its ability to inhibit Ply oligomerization. First, 100 nM (3 μg/ml) of Ply was incubated with 100 μM of PGG alone and were then mixed with erythrocytes. The membranes were then enriched by centrifugation and washed, and the proteins including the Ply complex, were dissolved to SDS-PAGE sample buffer without heating at 95°C. As a control, the proteins were incubated at 95°C to denature Ply and break the Ply complex completely. The proteins were separated in the SDS-PAGE gel (6 % gel). The monomeric Ply has an apparent MW of 55 kDa, whereas the oligomerized Ply runs as a high molecular complex migrating just underneath the separating gel (Figure 5B). As can be seen from the Coomassie-stained gel, the Ply complex was abolished with PGG and boiling at 95 °C. Sample containing only Ply contains the 55 kDa monomeric form. To reveal the minimum amount of PGG that can inhibit Ply oligomerization, dilution series of PGG were incubated with Ply, and the oligomerization was detected with SDS-PAGE and detection of Ply with Western blotting using the anti-His antibody (Figure 5C). The concentration that still inhibited Ply oligomerization was 30 μM. As a control, the dependence on the membrane cholesterol for Ply oligomerization, liposomes with varying mol-% (0 - 50) of cholesterol were incubated with Ply (Figure 5D). The results show that increasing concentrations of cholesterol above 20 mol-% induced Ply oligomerization.

Preprints (www.preprints.org) | NOT PEER-REVIEWED | Posted: 16 November 2020 doi:10.20944/preprints202011.0408.v1

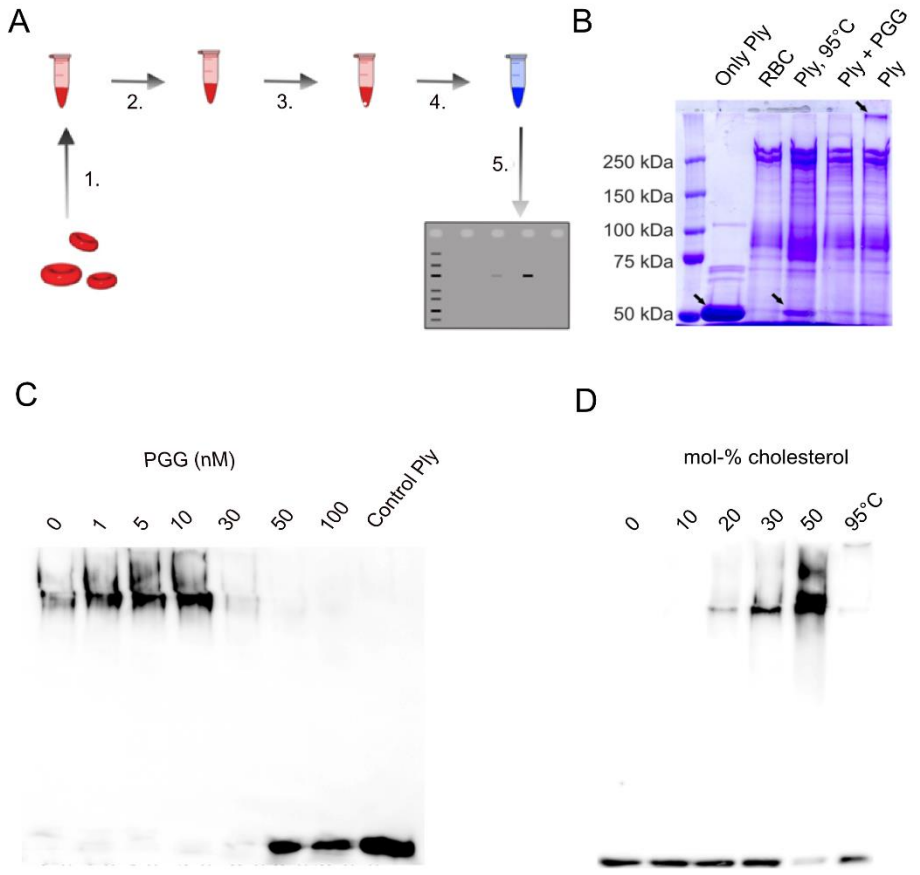

Figure 5. Pneumolysin oligomerization assay using erythrocytes. A. Scheme of the oligomerization assay. Erythrocytes suspended in phosphate buffer (1) were incubated with Ply causing lysis of the cells in the presence of different concentrations of PGG (2). The intact cells or membranes containing oligomerized Ply were centrifuged (3) and washed and were suspended into SDS-PAGE sample buffer (5), and the proteins were separated with SDS-PAGE. **B.** Coomassie blue -stained SDS-PAGE gel of erythrocyte membrane proteins and oligomerized Ply. Samples: Ply without incubation with erythrocytes, monomeric Ply; RBC, a control sample of erythrocytes incubated without Ply; Ply 95°C, erythrocytes incubated with Ply and the sample was heated at 95°C to depolymerize Ply oligomers; Ply + PGG, erythrocytes were mixed with Ply preincubated with PGG; Ply, erythrocytes incubated with Ply only, the high molecular weight oligomerized Ply complex indicated with a black arrow. **C.** Inhibition of Ply oligomerization by dilution series of PGG. Pneumolysin oligomers were detected with Western blotting using an anti-His antibody. Samples: MonoPly, a control of Ply without incubation with erythrocytes; Ply oligomers in the presence of PGG inhibitor concentrations (0 - 100 µM). **D.** Control experiment showing cholesterol dependence of Ply oligomerization using liposomes. Liposomes containing 0-50 mol-% of cholesterol were incubated with Ply, and the liposomes were solubilized into SDS-PAGE sample buffer, and Ply was detected with Western blotting as in **C.**

2.4. Inhibition of Ply cytotoxicity by PGG

The Ply cytotoxicity to lung pneumocyte A549 cells was analyzed by incubation of 2 nM of Ply with the cells grown in plastic wells (Figure 6). The cells remained bound to the wells during Ply treatment. The inhibition of PGG to pneumolysin cytotoxicity and LDH release by dead cells was measured as described in the methods. Lower concentrations of PGG (≤ 250 nM) caused a moderate inhibition whereas 500, 1000 and 2000 nM of PGG inhibited LDH release by 29, 76 and 89 % compared to the cells incubated with pneumolysin alone. Pneumolysin can induce cell death by three different pathways, e.g. apoptosis, programmed necroptosis, pyroptosis and direct cytotoxicity in a cell-type-specific manner [10,17]. Direct cytotoxicity of Ply released from *S. pneumoniae* has been shown to

Preprints (www.preprints.org) | NOT PEER-REVIEWED | Posted: 16 November 2020 doi:10.20944/preprints202011.0408.v1

cause cell death and LDH release of A549 cells [18]. The cells targeted by Ply have been shown to try to repair their cell membrane by the formation of Ply containing nanotubes, which subsequently form microvesicles that are shed of the membrane. [19]. Cell death is eventually caused by the leakage of calcium into the cell cytoplasm. Further studies will be required to clarify the role of PGG in inhibiting the cellular death mechanisms.

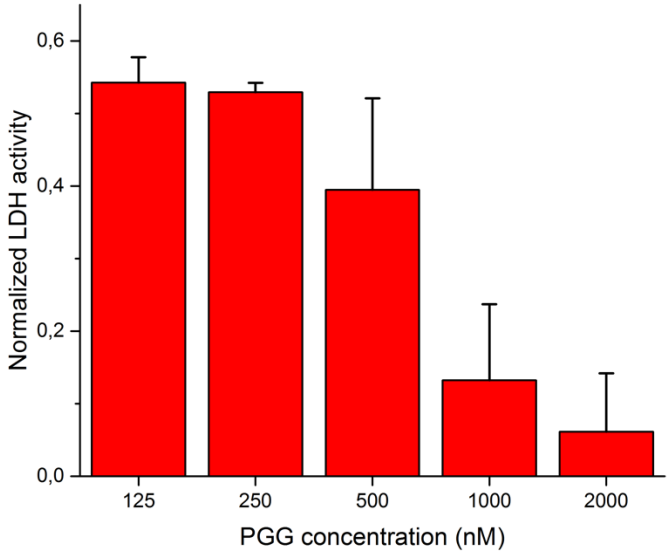

Figure 6. The inhibition of pneumolysin cytotoxicity with PGG. The cytotoxicity of Ply in the presence of PGG was quantitated with LDH cytotoxicity assay. The normalized LDH activities are shown as absorbance at 490 nm, averages of triplicate measurements are presented.

2.5. In silico studies of PGG interaction with Ply

According to the docking and energy minimization results, PGG binds to the pocket formed by domains 2, 3 and 4 (Figure 7). After energy minimization steps, some key amino acids in interactions are Glu42, Ser256, Asp257, Glu277 and Arg359 that hydrogen bonds to PGG. Similar interactions are also reported for EGCG, which was suggested to interact with Ser256, Glu277, Tyr358 and Arg359 in a former study [13]. After the simulation of 50 ns, PGG moved further from Asp257 and Ser256 but was still interacting with Glu42, Glu277 and Arg359.

According to the computational studies, the increased inhibitory power of PGG is based on the pentameric rotatable gallic acid-groups (Figure 7). Previously, epigallogatechin gallate (EGCG) was shown to inhibit Ply hemolytic activity, however micromolar concentrations were required for inhibition [13], which could be due to the lower number of free galloyl groups and thus weaker tannin nature of EGCG. This could also explain why vescalagin has much higher IC_{50} concentration for hemolysis inhibition than PGG, although they have the same number of aromatic rings. In PGG all galloyls are freely rotating and flexible while in vescalagin two of the galloyls are C-C linked to form a rigid HHDP group and the other three galloyls are linked to form the rigid NHTP group (Table 1, Figure 1). In contrast, gemin A and oenothein B have two galloyl groups not bonded together enabling a better binding affinity than for vescalagin (Figure 2). Oligomers in general are known to bind proteins more efficiently than the monomers [15]. The macrocyclic dimer oenothein B loses part of its potency, since the monomers are linked by two bonds thus losing the flexibility between the monomers. It is possible that the flexible dimer, gemin A could be able to bind to two Ply molecules, which would explain its better potency in causing precipitation in comparison to PGG and oenothein B.

Preprints (www.preprints.org) | NOT PEER-REVIEWED | Posted: 16 November 2020 doi:10.20944/preprints202011.0408.v1

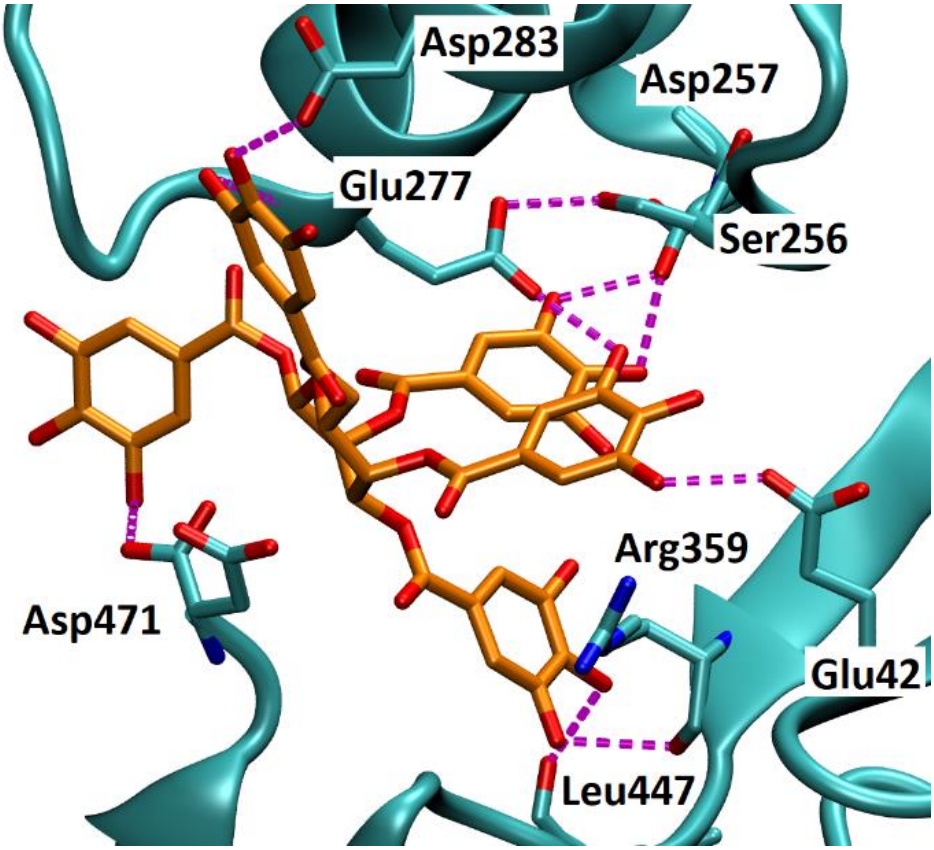

Figure 7. The binding mode of PLY-PGG. Possible hydrogen bond interactions are shown as dashed, purple lines. The binding orientation represents the docking conformation after energy minimization steps. Figure was prepared with VMD 1.9.2 [20].

(1)

3. Materials and Methods

3.1. Tannins

The structures of polyphenols studied are presented in Figure 1 and 2. They were purified and characterized as described in Engström et al. (2019). The compounds were dissolved to 10 % (v/v) ethanol-water solution.

3.2. Cloning and expression of recombinant pneumolysin

Pneumolysin gene was cloned with primers gacgacgacaagatggcaaataaagcagtaaatgac and gaggagaagcccggttta ctagtcattttctaccttatc. The DNA fragment was amplified with Phusion HotStart II DNA polymerase and was cloned into LIC-vector (LIC, ligation independent cloning) pET46EkLIC (Novagen) and the cloned insert was verified with sequencing. The bacteria were grown at 30°C, 250 rpm, to an OD600 of 0.6, and the protein expression was induced with 1.0 mM IPTG for 3.5 hours. Bacteria were harvested by centrifugation with 3000 x g, at +4°C and stored at -84°C. The recombinant protein was purified with Ni-NTA affinity chromatography. Briefly, bacteria were lysed with 0.2 mg/ml hen egg lysozyme (Sigma) in 50 mM sodium phosphate buffer pH 8.0, containing 0.5 M NaCl, EDTA-free protease inhibitor cocktail (Pierce), 20 mM imidazole, 20 µg/ml deoxyribonuclease and 1 mM $MgCl_2$ on ice for 30 mins. The lysate was sonicated to homogenize the cell debris further and was centrifuged at 20 000 x g, +4°C for 30 min. The filtered lysate was purified with Ni-NTA affinity

Preprints (www.preprints.org) | NOT PEER-REVIEWED | Posted: 16 November 2020 doi:10.20944/preprints202011.0408.v1

chromatography using HiPrep FF column using Äktaprime plus, GE Healthcare at +25°C. Further purification was done with gel filtration column HiLoad 16/60 Superdex 200 using Tris-Cl, pH 7.5, 0.15 M NaCl running buffer. The purity of the recombinant protein was analyzed with SDS-PAGE chromatography.

3.3. Hemolysis inhibition assays with tannins.

Native human erythrocytes were taken into EDTA-tubes. The erythrocytes were washed three times with PBS (0.15 M NaCl, 2.7 mM KCl, 8.1 mM Na_2HPO_4, 1.5 mM KH_2PO_4) by centrifugation with 700 x g, 10 min. The purified erythrocytes were stored at +4°C. Erythrocytes (1 % v/v) in PBS were mixed with 1 nM Ply and dilution series of polyphenol inhibitors in 96 well microtiter plates. The reaction was incubated for 30 min at 37°C. The plates were centrifuged, and the supernatant was pipetted into flat bottomed microtiter plates to measure the absorbance at 570 nm (VICTOR X4, PerkinElmer) of the released haemoglobin from lysed erythrocytes. The absorbances of triplicate measurements are presented as a function of inhibitor concentration. The IC_{50} values were calculated with Origin.

3.4. Precipitation assay

The precipitation assay with tannins was done as described previously with bovine serum albumin [15]. 10 μM of Ply and dilution series of polyphenols (5–1000 μM) were incubated in Na-acetate buffer (200 mM NaCl, 50 mM CH_3COONa, pH 5,0) at 25°C, 30 min with shaking. The reactions were carried out in Multiskan Ascent -plate reader (Labsystems) and the precipitation was measured at 414 nm.

3.5. Liposomes

Vesicles were prepared by dissolving 1 μM POPC (1-palmitoyl-2-oleoyl-glycero-3-phosphocholine, Avanti Polar lipids) and 1 - 50 mol-% cholesterol into chloroform : methanol (2:1, vol/vol). The solvent was evaporated with nitrogen, and the lipid film was hydrated into 10 mM Tris-Cl, 140 mM NaCl buffer for 30 min at 60 °C to a final concentration of 1000 μM. The lipid-buffer suspension was briefly vortexed followed by the extrusion procedure (Avanti mini extruder using 0.1 μm polycarbonate membranes filter, (Avanti Polar Lipids, Alabaster, AL, USA)) to form large unilamellar vesicles.

3.6. Oligomerization assay

100 nM Ply (3 μg), 1 % (v/v) erythrocytes and 100 μM PGG in PBS were incubated for 2 min at 25°C and were centrifuged 16 000 x g, 30 min at +7°C. The pellet containing intact erythrocytes and membranes from lysed cells were suspended into the water to complete the lysis and recentrifuged 16 000 x g, 30 min. The membranes were suspended into SDS-PAGE sample buffer (60 mM Tris-HCl pH 6,8; 2 % SDS; 0,001 % bromphenol blue; 0,5 % β-mercaptoethanol) without incubation at 95°C and the proteins were separated in 6 % SDS-PAGE gel. The gel was stained with Coomassie blue (40 % methanol; 10 % acetic acid; 0,25 % Briljant blue R-250) and destained in 20 % methanol, 5 % acetic acid overnight. The proteins were transferred to PVDF membrane for 30 min, 25 V in SDS-PAGE running buffer (25 mM Tris, 190 mM glycine, 0.1% SDS) using Trans-Blot Turbo Transfer System (Bio-Rad). The membrane was blocked with 5 % (w/v) defatted milk powder in TBS-Tween (10 mM Tris pH 7,5; 150 mM NaCl; 0,05 % Tween-20) for 30 min at 25°C. The His-tagged Ply was detected with anti-His antibody (1:5000 -dilution, Sigma-Aldrich) and HRP-labelled anti-mouse antibody (1:10 000 -dilution, DakoCytomation). After washing the membrane was incubated with ECL detection substrate (WesternBright Quantum, Labtech) and was imaged using ImageQuant LAS 4000 (GE Healthcare).

3.7. A549 cell cytotoxicity assay

Preprints (www.preprints.org) | NOT PEER-REVIEWED | Posted: 16 November 2020 doi:10.20944/preprints202011.0408.v1

5000 cells/well of A549-cells were grown in DMEM, 2 mM glutamine, 10 % FCS for 48 h in 96-well microtiter wells. Cells were washed with PBS and dilutions of PGG (0, 125, 250, 500, 1000 and 2000 nM) and 2 nM Ply in PBS were added to the wells and incubated for 2 h at 37 °C, 5 % CO_2. The Ply cytotoxicity was determined with Cytotoxicity Detection Kit^{PLUS} (Roche) according to manufacturer's instructions. The released LDH was measured at A_{490}. Complete lysis control was measured in the presence of 0.02 % Triton X-100, and for background hemolysis measurements, RBC were incubated without Ply. The values were normalized by calculating using the equation ($A_{490\ Ply+inhibitor} - A_{490\ Background}$) / ($A_{490\ Triton\ X-100} - A_{490\ Background}$).

3.8. Molecular modelling

PGG was converted to 3D SYBYL MOL2 format containing OPLS3 partial charges with LIGPREP in MAESTRO 2018-1 (Schrödinger, LLC, New York, NY, USA, 2018) and considering the protonation at pH 7.4. Target structure preparation of PLY X-ray structure (PDB code 5CR6 [5]) was performed with Protein Preparation Wizard in MAESTRO at pH 7.4 using default settings. Extra Precision (XP) mode of GLIDE [21,22] was used to dock PGG between PLY domains 2, 3 and 4 (centroid coordinates 4.337, 21.215, 220.177).

For molecular dynamic simulations, PGG was parametrized with ANTECHAMBER 17 [23] using AM1-bcc charge method. Tleap in AMBER 18 package (University of California, San Francisco, Case et al., 2018) was used to parametrize protein with ff14SB force field [24], combine protein-ligand complex, add hydrogen atoms and solvate the system with a rectangular box of transferable intermolecular potential three-point (TIP3P) water molecules [25] extending 13 Å in every direction around the solute. The system was neutralized by adding Na+ counter ions. 50 ns simulation was run with NAMD2.13 [20,26] in four steps: 1) 15,000 steps of energy minimization with restrained Ca atoms (5 kcal/mol); 2) 15,000 steps of energy minimization without restraints; 3) 180,000 steps molecular dynamics simulation with restrained Ca atoms (5 kcal/mol); 4) 25,000,000 (50 ns) steps of simulation without restraints.

4. Conclusions

In summary, we have shown the specific inhibition of Ply by hydrolyzable tannins containing polyvalent galloyl groups using cellular models, i.e. inhibition of Ply induced hemolysis and cytotoxicity to A549 cells. The structure-function relationship of Ply – tannin interaction was determined by hemolysis inhibition and by the direct precipitation of Ply by tannins. The interaction of Ply with PGG was modelled with docking experiments. The efficient and specific inhibition by PGG is suggested to rely on the interaction between the phenolic hydroxy-groups of PGG and Ply polar amino acids situated in the pocket formed by domains 2, 3 and 4. PGG abolished the Ply complex formation on the surface of erythrocytes as shown by Western blotting of the solubilized erythrocyte membranes treated with recombinant Ply. The structural features reveal that (1) hydrolyzable tannin monomers such as PGG and tellimagrandin II with a good number of polyvalent and flexible galloyl groups, as well as (2) galloyl-containing oligomers consisting of glucopyranose-based monomers with non-macrocyclic linkage, have strongest inhibitory powers and are thus potential therapeutic compounds to inhibit Ply cytotoxicity.

Author Contributions: Conceptualization, JPS and SH; investigation, SM, SK, MTE.; writing—original draft preparation, SH; writing—review and editing, JPS, OP; supervision, SH, JPS., OP; All authors have read and agreed to the published version of the manuscript.

Funding: The hydrolysable tannins were purified during the OptiFeed project that was funded by the Academy of Finland (grant no 298177 to JPS).

Acknowledgements: We thank professor Markku Koulu for encouragement and support for the project.

Conflicts of Interest: The authors declare no conflict of interest."

Appendices

Preprints (www.preprints.org) | NOT PEER-REVIEWED | Posted: 16 November 2020 doi:10.20944/preprints202011.0408.v1

Table A1. Screening of tannin compounds with hemolysis assays. IC_{50} values were estimated from the inhibition curves. Compounds taken for more detailed analysis are highlighted with yellow.

Compound	MW (Da)	IC_{50} (nM)
1,2,3,4,6-penta-*O*-galloyl-β-D-glucose	940,67	10
tellimagrandin II	938,66	10
gemin A	1873,28	20
lambertianin C	2805,9	20
sanguiin H-6	1871,27	20
agrimoniin	1871,27	30
gallotannin mixture	1396.99*	40
casuarictin	936,64	40
oenothein A	2353,62	40
salicarinin B	1869,25	50
oenothein B	1569,08	60
tellimagrandin I	786,55	60
punicalagin	1084,71	60
1,2,-di-*O*-galloyl-4,6-HHDP-β-D-glucose	786,55	70
salicarinin A	1869,25	80
castalagin	934,63	80
casuarinin	936,64	90
geraniin	952,64	100
salicarinin C	1869,25	100
stachyurin	936,64	>100
pedunculagin	784,54	>100
vescalagin	934,63	>100
castavaloninic acid	1102,73	>100
chebulagic acid	954,66	>100
vescavaloninic acid	1102,73	>100
chebulinic acid	956,67	>100
1-*O*-galloyl-β-D-glucose	332,26	>100

*Molecular weight of the gallotannin mixture presented based on octagalloylglucose

References

1. Weiser, J.N.; Ferreira, D.M.; Paton, J.C. *Streptococcus pneumoniae*: transmission, colonization and invasion. *Nat. Rev. Microbiol.* **2018**, *16*, 355–367, doi:10.1038/s41579-018-0001-8.
2. Feldman, C.; Anderson, R. The Role of *Streptococcus pneumoniae* in Community-Acquired Pneumonia. *Semin. Respir. Crit. Care Med.* **2016**, doi:10.1055/s-0036-1592074.
3. Mehr, S.; Wood, N. *Streptococcus pneumoniae* - a review of carriage, infection, serotype replacement and vaccination. *Paediatr. Respir. Rev.* 2012.
4. Gilbert, R.J.C. Chapter 5: Cholesterol-dependent cytolysins. In *Advances in experimental medicine and*

biology; 2010.

5. Marshall, J.E.; Faraj, B.H.A.; Gingras, A.R.; Lonnen, R.; Sheikh, M.A.; El-Mezgueldi, M.; Moody, P.C.E.; Andrew, P.W.; Wallis, R. The crystal structure of pneumolysin at 2.0Å resolution reveals the molecular packing of the pre-pore complex. *Sci. Rep.* **2015**, doi:10.1038/srep13293.
6. Guiral, S.; Mitchell, T.J.; Martin, B.; Claverys, J.P. Competence-programmed predation of noncompetent cells in the human pathogen *Streptococcus pneumoniae*: genetic requirements. *Proc. Natl. Acad. Sci. U. S. A.* **2005**, *102*, 8710–8715, doi:0500879102 [pii]; 10.1073/pnas.0500879102 [doi].
7. Bandara, M.; Skehel, J.M.; Kadioglu, A.; Collinson, I.; Nobbs, A.H.; Blocker, A.J.; Jenkinson, H.F. The accessory Sec system (SecY2A2) in *Streptococcus pneumoniae* is involved in export of pneumolysin toxin, adhesion and biofilm formation. *Microbes Infect.* **2017**, doi:10.1016/j.micinf.2017.04.003.
8. Price, K.E.; Camilli, A. Pneumolysin localizes to the cell wall of *Streptococcus pneumoniae*. *J. Bacteriol.* **2009**, doi:10.1128/JB.01489-08.
9. Anderson, R.; Feldman, C. Pneumolysin as a potential therapeutic target in severe pneumococcal disease Introduction: the burden of pneumococcal infection. *J. Infect.* **2017**, doi:10.1016/j.jinf.2017.03.005.
10. Nishimoto, A.T.; Rosch, J.W.; Tuomanen, E.I. Pneumolysin: Pathogenesis and Therapeutic Target. *Front. Microbiol.* 2020.
11. Zafar, M.A.; Wang, Y.; Hamaguchi, S.; Weiser, J.N. Host-to-Host Transmission of *Streptococcus pneumoniae* Is Driven by Its Inflammatory Toxin, Pneumolysin. *Cell Host Microbe* **2017**, doi:10.1016/j.chom.2016.12.005.
12. Quideau, S.; Deffieux, D.; Douat-Casassus, C.; Pouységu, L. Plant polyphenols: Chemical properties, biological activities, and synthesis. *Angew. Chemie - Int. Ed.* 2011.
13. Song, M.; Teng, Z.; Li, M.; Niu, X.; Wang, J.; Deng, X. Epigallocatechin gallate inhibits *Streptococcus pneumoniae* virulence by simultaneously targeting pneumolysin and sortase A. *J. Cell. Mol. Med.* **2017**, doi:10.1111/jcmm.13179.
14. Salminen, J.P.; Karonen, M.; Sinkkonen, J. Chemical ecology of tannins: Recent developments in tannin chemistry reveal new structures and structure-activity patterns. *Chem. - A Eur. J.* **2011**, doi:10.1002/chem.201002662.
15. Engström, M.T.; Arvola, J.; Nenonen, S.; Virtanen, V.T.J.; Leppä, M.M.; Tähtinen, P.; Salminen, J.P. Structural Features of Hydrolyzable Tannins Determine Their Ability to Form Insoluble Complexes with Bovine Serum Albumin. *J. Agric. Food Chem.* **2019**, doi:10.1021/acs.jafc.9b02188.
16. Leppä, M.M.; Karonen, M.; Tähtinen, P.; Engström, M.T.; Salminen, J.P. Isolation of chemically well-defined semipreparative liquid chromatography fractions from complex mixtures of proanthocyanidin oligomers and polymers. *J. Chromatogr. A* **2018**, doi:10.1016/j.chroma.2018.09.034.
17. Paton, J.C.; Kim, J.-Y.; Rhee, D.-K.; Briles, D.E.; Pyo, S. *Streptococcus pneumoniae* induces pyroptosis through the regulation of autophagy in murine microglia. *Oncotarget* **2015**, doi:10.18632/oncotarget.6592.
18. Jacques, L.C.; Panagiotou, S.; Baltazar, M.; Senghore, M.; Khandaker, S.; Xu, R.; Bricio-Moreno, L.; Yang, M.; Dowson, C.G.; Everett, D.B.; et al. Increased pathogenicity of pneumococcal serotype 1 is driven by rapid autolysis and release of pneumolysin. *Nat. Commun.* **2020**, doi:10.1038/s41467-020-15751-6.
19. Wolfmeier, H.; Radecke, J.; Schoenauer, R.; Koeffel, R.; Babiychuk, V.S.; Drücker, P.; Hathaway, L.J.; Mitchell, T.J.; Zuber, B.; Draeger, A.; et al. Active release of pneumolysin prepores and pores by mammalian cells undergoing a *Streptococcus pneumoniae* attack. *Biochim. Biophys. Acta - Gen. Subj.* **2016**, doi:10.1016/j.bbagen.2016.07.022.
20. Humphrey, W.; Dalke, A.; Schulten, K. VMD: Visual molecular dynamics. *J. Mol. Graph.* **1996**, doi:10.1016/0263-7855(96)00018-5.

 doi:10.20944/preprints202011.0408.v1

21. Friesner, R.A.; Banks, J.L.; Murphy, R.B.; Halgren, T.A.; Klicic, J.J.; Mainz, D.T.; Repasky, M.P.; Knoll, E.H.; Shelley, M.; Perry, J.K.; et al. Glide: A New Approach for Rapid, Accurate Docking and Scoring. 1. Method and Assessment of Docking Accuracy. *J. Med. Chem.* **2004**, doi:10.1021/jm0306430.
22. Halgren, T.A.; Murphy, R.B.; Friesner, R.A.; Beard, H.S.; Frye, L.L.; Pollard, W.T.; Banks, J.L. Glide: A New Approach for Rapid, Accurate Docking and Scoring. 2. Enrichment Factors in Database Screening. *J. Med. Chem.* **2004**, doi:10.1021/jm030644s.
23. Wang, J.; Wang, W.; Kollman, P. a; Case, D. a Antechamber, An Accessory Software Package For Molecular Mechanical Calculations. *J. Am. Chem. Soc* **2001**.
24. Maier, J.A.; Martinez, C.; Kasavajhala, K.; Wickstrom, L.; Hauser, K.E.; Simmerling, C. ff14SB: Improving the Accuracy of Protein Side Chain and Backbone Parameters from ff99SB. *J. Chem. Theory Comput.* **2015**, doi:10.1021/acs.jctc.5b00255.
25. Jorgensen, W.L.; Chandrasekhar, J.; Madura, J.D.; Impey, R.W.; Klein, M.L. Comparison of simple potential functions for simulating liquid water. *J. Chem. Phys.* **1983**, doi:10.1063/1.445869.
26. Phillips, J.C.; Braun, R.; Wang, W.; Gumbart, J.; Tajkhorshid, E.; Villa, E.; Chipot, C.; Skeel, R.D.; Kalé, L.; Schulten, K. Scalable molecular dynamics with NAMD. *J. Comput. Chem.* 2005.